

# Delayed response of global ionospheric electron content to EUV variations derived from combined SolACES-SDO/EVE measurements

Christoph Jacobi<sup>1</sup>, Claudia Unglaub<sup>1</sup>, Gerhard Schmidtke<sup>2</sup>,  
Robert Schäfer<sup>2</sup>, Norbert Jakowski<sup>3</sup>

<sup>1</sup>*Institute for Meteorology, Universität Leipzig*

<sup>2</sup>*Fraunhofer-Institut für Physikalische Messtechnik (IPM), Freiburg*

<sup>3</sup>*German Aerospace Center, Neustrelitz*

## Summary

The ionospheric response to solar EUV variability during 2011 - 2014 is shown by an EUV proxy based on primary ionization calculations using combined solar spectra from SDO/EVE and SolACES on board the ISS. The daily proxies are compared with global mean TEC analyses. At time scales of the solar rotation and longer, there is a time lag between EUV and TEC variability of about one to two days, indicating dynamical processes in the thermosphere/ionosphere systems. This lag is not seen at shorter time scales. When taking this delay into account the TEC variance at the seasonal and short-term time scale explained by EUV variations increases from 71% to 76%.

## Zusammenfassung

Die ionosphärische Antwort auf Variationen des solaren EUV im Zeitraum 2011-2014 wird anhand eines Proxys dargestellt, welcher die primäre Ionisation auf der Basis gemessener solare EUV-Spektren beinhaltet. Die täglichen Werte werden mit Analysen des global gemittelten Gesamtelektronengehalts verglichen. Auf Zeitskalen der solaren Rotation und länger findet sich eine Zeitverzögerung zwischen der EUV-Variation und des derjenigen des Gesamtelektronengehalts von ein bis 2 Tagen, welche auf dynamische Prozesse im System Thermosphäre/Ionosphäre hinweist. Die Verzögerung ist auf kurzen Zeitskalen nicht zu sehen. Wenn diese Verzögerung berücksichtigt wird, erhöht sich die durch EUV-Variationen erklärte Varianz des Elektronengehalts von 71% auf 76%.

## 1. Introduction

The solar extreme ultraviolet (EUV) radiation varies on different time scales, including the 27-day Carrington rotation as one of the primary sources of variability at the intra-seasonal time scale. Consequences are strong changes of ionization of the Earth's upper atmosphere, and corresponding variability of the electron density and also the Total Electron Content (TEC, frequently given in terms of TEC Units,  $1 \text{ TECU} = 10^{16} \text{ electrons/m}^2$ ). The majority of electrons are found in the ionospheric F layer where, according to the Chapman theory, electron production is proportional to

the ionizing EUV intensity, and electron density is approximately proportional to the electron production rate. Therefore, TEC variability is a coarse estimate for ionization as well, so that indices describing ionization may be compared against ionospheric TEC or, in turn, these indices may be used to provide a first guess of ionospheric TEC variability. Therefore, Unglaub et al. (2011, 2012) has introduced a proxy, termed EUV-TEC, which is based on the vertical and globally integrated primary ionization rates calculated from spectral EUV fluxes measured by satellite instruments such as TIMED/SEE (Woods et al., 2000, 2005). They found that, using data of about one decade, simple primary ionization calculations based on the measured spectra describe the TEC variability better than e.g. F10.7.

However, correlation of parameters describing ionospheric electron density and EUV proxies is not always strong at time scales of the solar rotation, and several studies report a delayed response of the ionospheric plasma density to solar activity changes (e.g. Jakowski et al., 1991; Astafyeva et al., 2008; Afraimovich et al., 2008; Lee et al., 2012). In most cases, TEC is reported to be delayed against the variation of the solar radiation by 1-2 days. To interpret the ionospheric delay, Jakowski et al. (1991) performed simplified theoretical studies using a one-dimensional numerical model. They found a delayed accumulation of atomic oxygen at 180 km height caused by slow diffusion of atomic oxygen that has been created via O<sub>2</sub> photo-dissociation. Since the major F region ionization is proportional to O, these results were consistent with the observed delayed ionospheric ionization response.

In this paper, we shall make an attempt to improve the performance of the EUV-TEC proxy after Unglaub et al. (2011, 2012) by taking into account the ionospheric delay mentioned above. We shall apply EUV spectra from combined SDO/EVE and SolACES measurements from 2011 through early spring 2014, and modify the EUV-TEC proxy through shifting the spectral contributions at the solar rotation time scale by the observed delay.

## 2. EUV data and analysis

The Solar Dynamics Observatory (SDO) was launched on 11 February 2010 (Pesnell et al., 2012), and data are available from 1 May 2010. The Extreme Ultraviolet Variability Experiment (EVE) onboard SDO measures the solar EUV irradiance from 0.1 to 105 nm with a spectral resolution of 0.1 nm, a temporal cadence of ten seconds, and an accuracy of 20% (Woods et al., 2012). SolACES (Schmidtke et al., 2006, 2014) is recording the short-wavelength solar EUV irradiance from 16.5 to 150 nm since 2008. The mission is extended from a period of 18 months to more than 8 years until end of 2016. SolACES is operating three grazing incidence planar grating spectrometers and two three-current ionization chambers. Re-filling the ionization chambers with different gases repeatedly and using overlapping band-pass filters the absolute EUV fluxes are derived in these spectral intervals. This provides an independent and absolute measurement of EUV fluxes that are used to calibrate the SolACES spectrometers. This way the problem of continuing efficiency changes in space-born instrumentation, which otherwise cannot be corrected without specific effort, is overcome during the mission.

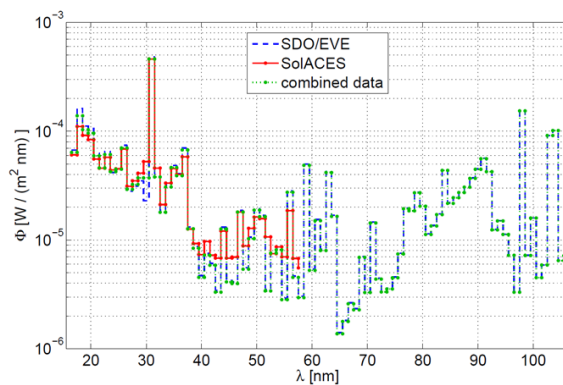


Figure 1: Example of SDO/EVE and SolACES spectra, and combined spectrum.

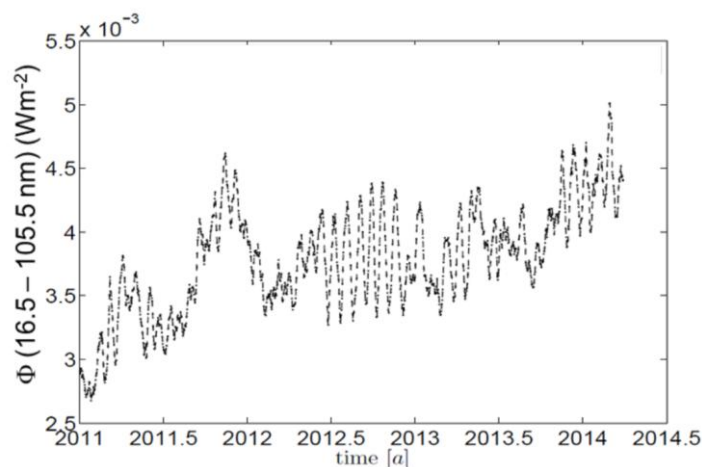


Figure 2: Solar flux between 16.5 nm and 105.5 nm from combined SDO/EVE and SolACES SSI measurements.

To calculate combined spectra, SDO/EVE version 4 daily spectra are used together with SolACES spectra. Between 16.5 and 29.5 nm the spectral fluxes are averaged, when SolACES spectra are available. A correction factor for SDO/EVE was then determined for each of these days by linearly fitting the ratio of the SDO/EVE integrated flux to the mean SDO/EVE and SolACES integrated flux between 16.5 and 29.5 nm. Thus the correction/weighting factor linearly scales from its initial value applied at 29.5 nm to unity at 105.5 nm. The correction factor changes, owing to the respective performance of the two instruments which changes with time. If no SolACES observation is available, the correction factor is derived from the fit function by interpolation to the particular day and applied to the SDO/EVE measurements between 16.5 and 29.5 nm. For wavelengths beyond 29.5 nm, the spectra solely consist of SDO/EVE-data, weighted with the correction factor. Figure 1 shows an example of SDO/EVE and SolACES spectra, with a correction factor in this case very close to unity, and the resulting combined spectrum. Figure 2 presents the time series of combined EUV fluxes integrated from 16.5 – 105.5 nm from January 2011 through March 2014. The dataset covers part of the increasing phase of solar cycle 24, and the variability of EUV is also characterized by the 27-day solar rotation, particularly well expressed during the 2<sup>nd</sup> half of 2012.

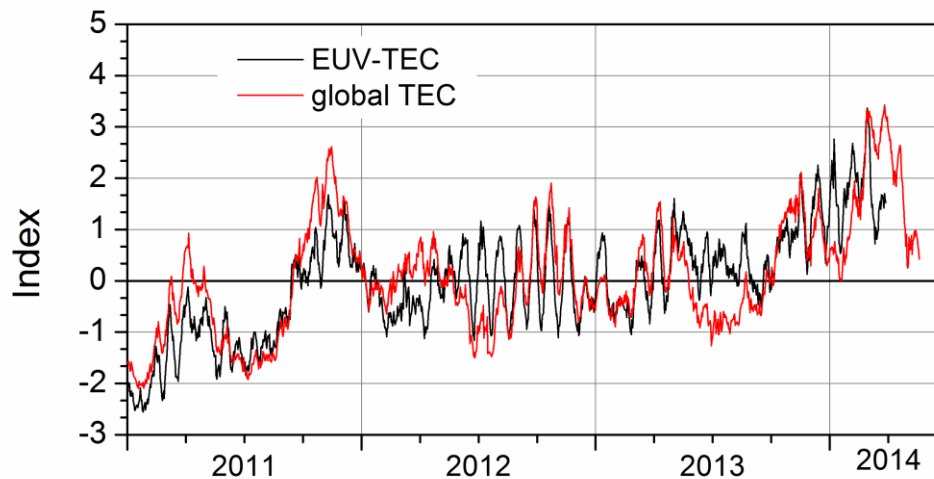


Figure 3: Times series of normalized global mean ionization rates (EUV-TEC proxy, red) and normalized global TEC (black).

We analyze the EUV-TEC proxy after Unglaub et al. (2011, 2012), based on the combined SDO/EVE-SolACES between 16.5 and 105.5 nm. EUV-TEC is calculated from the satellite-borne EUV measurements assuming a model atmosphere that consists of four major atmospheric constituents. Regional number densities of the background atmosphere are taken from the NRLMSISE-00 model (Picone et al., 2002). Daily global mean TEC values have been calculated based on IGS TEC maps (Hernandez-Pajares et al., 2009) in order to evaluate the EUV-TEC proxy, and they will be used here to analyze the ionospheric delay. The resulting ionization rates and global TEC values were normalized by subtracting the mean and dividing by the standard deviation from January 20, 2011 through March 10, 2014 (approx. Carrington rotations 2106 - 2147). The mean values and standard deviations are  $1.180 \cdot 10^{19} \pm 1.23 \cdot 10^{18}$  ions/m<sup>2</sup> for the ionization rates, and  $24.41 \pm 6.05$  TECU for global TEC. The corresponding time series are shown in Figure 3. Their variability is generally similar, although not identical, and also corresponds to the one of the EUV flux in Figure 2.

In order to analyze the correlation of TEC and EUV-TEC at different time scales, we filtered the normalized data using a Lanczos bandpass filter with 100 weights. In Figure 4, EUV-TEC and TEC for several period bands are presented. The upper panel (a) shows the data for all time scales up to 3 months. The correlation coefficient between normalized TEC and EUV-TEC at these time scales is  $r = 0.844$  ( $r^2 = 0.712$ ). Other analyses (Unglaub et al., 2011) provided greater correlation coefficients, but these included the 11-year cycle. Longer time scales will not be considered here, because these are dominated by the annual cycle, which is different for TEC and solar radiation, and part of the 11-year cycle. The next two panels of Figure 4 show the EUV-TEC and TEC variations at period intervals 17-53 days (including the solar rotation) and 54-76 days. One can see from Figure 4b, which mainly exhibits the 27-day solar rotation that there is a delay of TEC frequently visible when the amplitude of the 27-day cycle is well expressed. For longer time scales (Figure 4c), the lag is also visible, but more irregular albeit larger in those cases it appears. The last panel (d) of Figure 4

shows the residuals, i.e. the differences between the curves in panel (a) and those in panels (b) and (c). Those values are representative for short-term fluctuations and long ones with time scales of 77-90 days. The variations are more irregular, and the correlation between EUV-TEC and TEC is weak at these time scales.

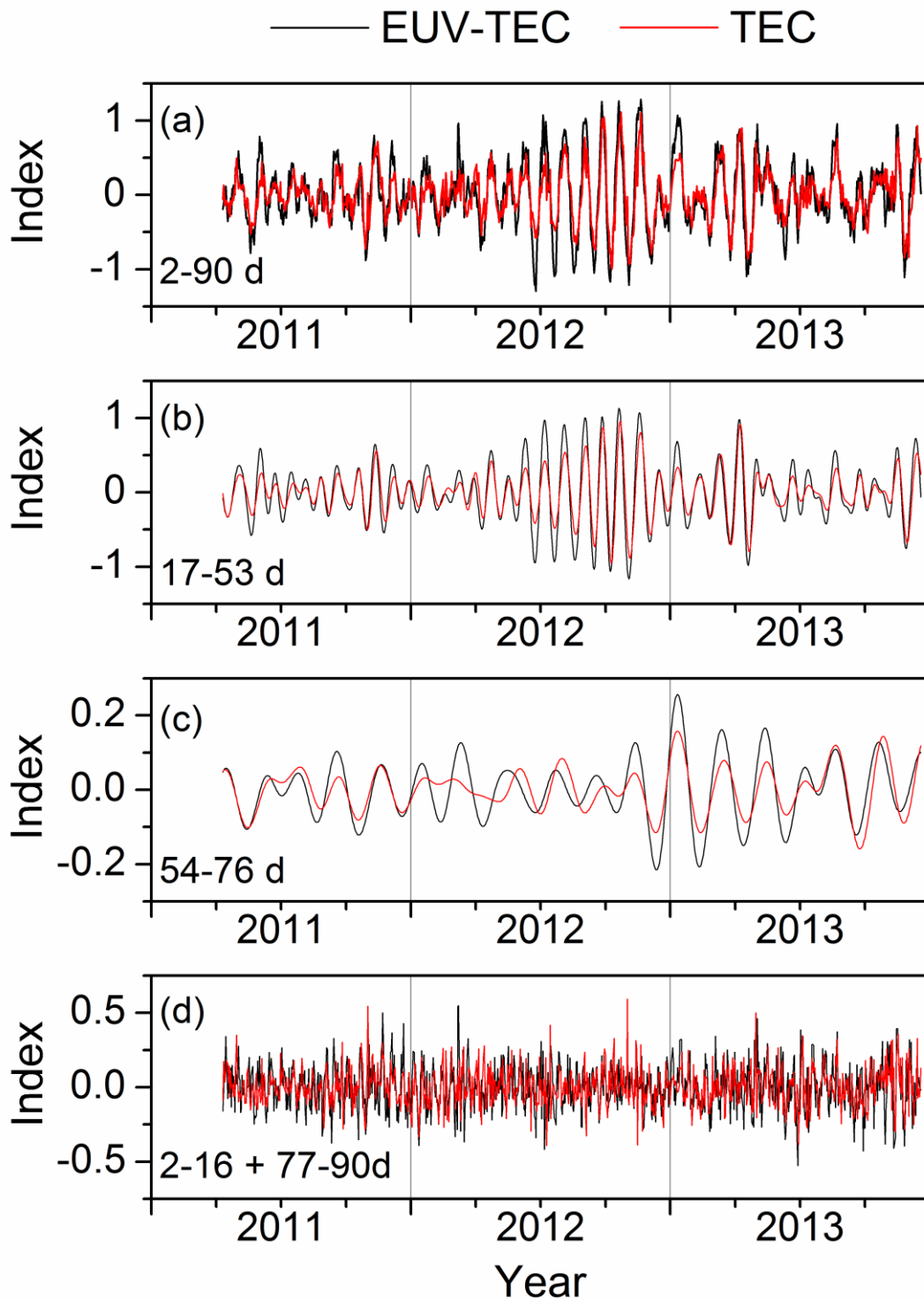


Figure 4: Time series of EUV-TEC and global TEC in different period bands (a) 0-90 days (b) 17-53 days (c) 54-76 days (d) 2-17 and 77-90 days.

To systematically investigate the delay at different time scales, we now filtered the time series and the cut-off periods of the Lanczos filter were chosen in such a way that each period band ranges over 4 days, while the centre of the period band was shifted from 4 to 88 days. For each pair of filtered time series, i.e. for each time scale (which was defined as the centre of the respective period window), the cross-correlation function was calculated. The results are shown in Figure 5. Positive values indicate that TEC variations lag EUV ones. Solid dots are added that show the time lag with maximum correlation which can, however, only be provided at an accuracy of one day. Figure 5 shows that at short time scales of few days, the correlation is weak, and the ionospheric delay is small. At time scales of the solar rotation, the strongest correlation is found and global TEC lags EUV-TEC variations by about one day. The lag increases to 2 days for time scales around 2 months, such that the lag scales with the time scale of the variation, which would be consistent with slow transport processes being responsible for ionospheric delay.

### 3. Considering the ionospheric delay in EUV-TEC

To improve the correlation between TEC and EUV-TEC, we constructed a new index from the original one, which takes into account the time lag at the respective time scales of the EUV variations. To this end, we filtered the EUV-TEC time series in different period windows, shifted the filtered series using the time lags taken from Figure 5, and reconstructed the EUV-TEC series from these values. Taking into account that the time resolution of the datasets allows only a first and coarse approach, we did not consider small structures in the time lag, but used a period window of 17-53 days that was shifted by 1 day and another window of 54-76 days that was shifted by 2 days.

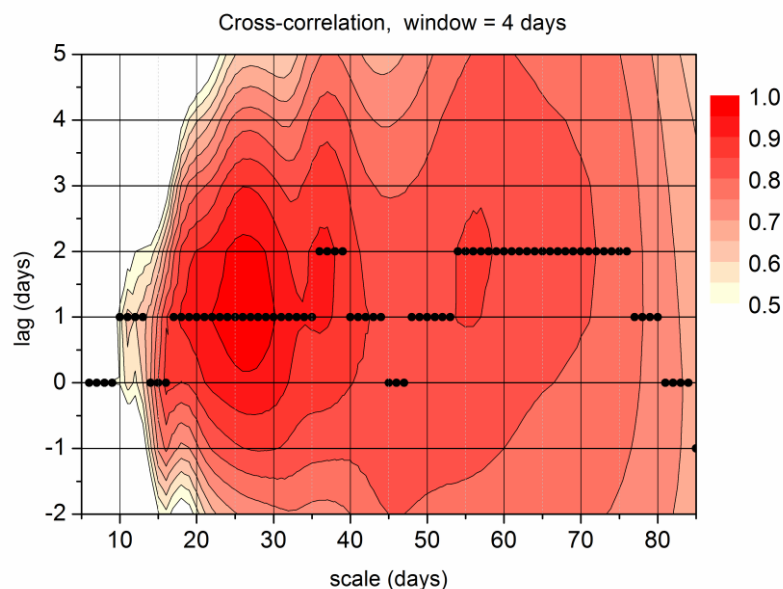


Figure 5: Cross-correlation coefficients between global TEC and EUV-TEC based on SDO/EVE and SolACES combined daily EUV spectra. The scale is the centre of the 4-day period band of the respective filter. Positive values indicate that TEC variations lag EUV ones. Solid dots show the lag with maximum correlation at an accuracy of one day.

Figure 6 shows an example of the original EUV-TEC index, the modified one, and the normalized TEC time series. The ionospheric delay between TEC and EUV-TEC is clearly visible with the original data, but vanishes if the modification is applied. Short-term variations are retained. When using the modified EUV-TEC time series, the correlation between normalized TEC and EUV-TEC increases to  $r = 0.874$  ( $r^2 = 0.764$ ), i.e. the TEC variance explained by the EUV-TEC proxy has increased by about 5%. The respective scatter plots are shown in Figure 7. One can see that after modification the scatter has decreased.

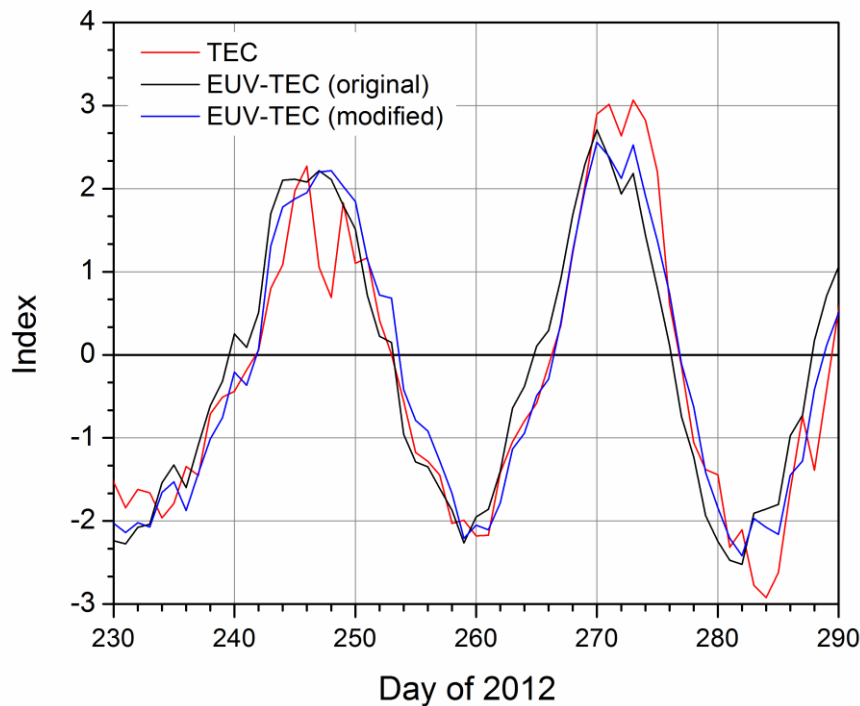


Figure 6: Example of normalized TEC, EUV-TEC, and EUV-TEC modified by shifting the filtered contributions in the 17-53 day range by 1 and in the 54-77 day range by 2 days.

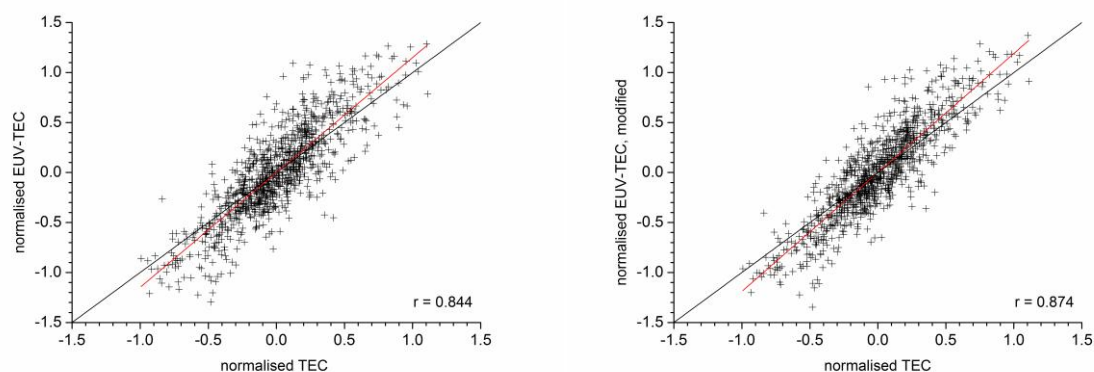


Figure 7: Normalized EUV-TEC vs. TEC. Left panel: original EUV-TEC. Right panel: Modified EUV-TEC.

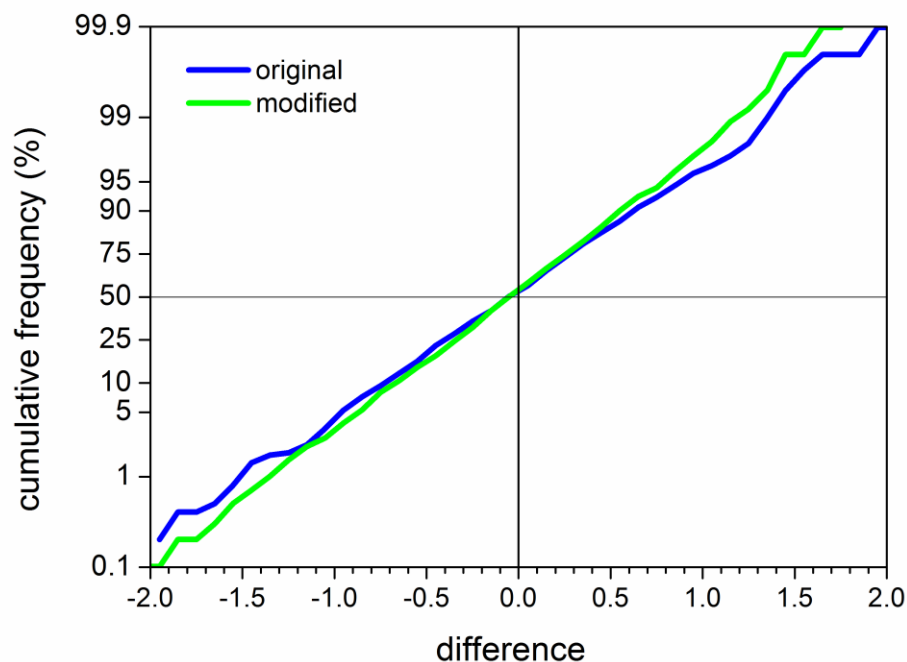


Figure 8: Cumulative frequency distribution of differences between normalized global TEC and original (blue) or modified (green) EUV-TEC index. Positive differences indicate larger normalized TEC.

To further visualize the improvement, we calculated the differences between normalized global TEC and the EUV-TEC index (at time scales to 3 months, i.e. high-pass filtered with a cut-off period of 90 days) both using the original values and the modified EUV-TEC. While the unfiltered EUV-TEC and TEC data shown in Figure 3 had been scaled to a standard deviation of 1, after the filtering their mean amplitudes differ slightly. Therefore the input data used to calculate the differences have been again scaled to a standard deviation of 1 to allow of comparability. Then the standard deviations of the differences between scaled TEC and EUV-TEC decreases from 0.56 for the original EUV-TEC to 0.50 for the modified one. Figure 8 shows the cumulative frequency distribution of the differences. One can see that the line for the original data starts at larger differences and also ends at larger differences, i.e. after modification especially the large differences between TEC and EUV-TEC appear more rarely.

#### 4. Conclusions and outlook

When taking into account the ionospheric delay at the solar rotation time scale, proxies to describe the influence of EUV on ionization rates can be improved. It should be stated here that the ionization rates calculated by the EUV-TEC model represent only a coarse description of global TEC, and only about  $\frac{3}{4}$  of the variance at the intra-seasonal time scale are explained. At the decadal time scale, the correlation increases to about  $r = 0.95$  (Unglaub et al., 2012), but this is mainly owing to the 11-year Schwabe cycle. The EUV-TEC model also does not account for dynamics, secondary ionization, or ionization through electron precipitation at higher latitudes. It also does not take into account effects of ionospheric storms, which are a challenge for TEC forecast



(Borries et al., 2015). Nevertheless, EUV-TEC describes TEC variations better than conventional indices like F10.7 (Unglaub et al., 2011) and thus may be useful as a proxy for EUV and to replace F10.7 e.g. in models where it is used as input data. Taking into account the time delay will further improve the EUV-TEC proxy.

Obviously, the results presented here are preliminary. Further analyses will employ SDO/EVE version 5 data which recently had become available. Furthermore, the EUV spectral data set will be extended using TIMED/SEE data in order to cover a full solar cycle. We used daily EUV spectra and daily and global averaged TEC, which gives only coarse values for the time lag. TEC maps are available at higher temporal resolution, and EUV fluxes at least for some spectral bands are also available e.g. from SDO, SOHO/SEM (Judge et al., 1998) or GOES. This provides the possibility to study ionospheric delay in higher temporal resolution and spatially resolved, however, for the calculation of the EUV-TEC index spectral resolution is required, so that this would only provide guidance for further improvements.

Taking into account the ionospheric delay by simply shifting the contributions from the respective period ranges also neglects possible processes taking place during the 1-2 days such as the O production from O<sub>2</sub> dissociation and subsequent modifications in the EUV absorption. Further analyses will take into account possible weighting of the shifted contributions, and this also will require modeling of the photodissociation and transport processes to estimate these weights.

## Acknowledgements

EVE version 4 spectra have kindly been provided by LASP, University of Colorado at Boulder. TEC data has been provided by NASA through ftp access on <ftp://cddis.gsfc.nasa.gov/gps/products/ionex/>.

## References

- Afraimovich, E.L., Astafyeva, E.I., Oinats, A.V., Yasukevich, Yu.V., Zhivetiev, I.V., 2008: Global electron content: a new conception to track solar activity. *Ann. Geophys.*, 26, 335–344.
- Astafyeva, E.I., Afraimovich, E.L., Oinats, A.V., Yasukevich, Yu.V., Zhivetiev, I.V., 2008: Dynamics of global electron content in 1998–2005 derived from global GPS data and IRI modeling. *Adv. Space Res.*, 42, 763–769.
- Borries, C., Berdermann, J., Jakowski, N., Wilken, V., 2015: Ionospheric storms - a challenge for empirical forecast of the Total Electron Content. *J. Geophys. Res. Space Phys.*, doi: 10.1002/2015JA020988.
- Hernandez-Pajares, M., Juan, J.M., Sanz, J., Orus, R., Garcia-Rigo, A., Feltens, J., Komjathy, A., Schaer, S.C., Krankowski, A., 2009: The IGS VTEC maps: a reliable source of ionospheric information since 1998, *J. Geod.* 83, 263–275.
- Jakowski, N., Fichtelmann, B., Jungstand, A., 1991: Solar activity control of ionospheric and thermospheric processes. *J. Atmos. Terr. Phys.*, 53, 1125-1130.
- Judge, D.L., McMullin, D.R., Ogawa, H.S., Hovestadt, D., Klecker, B., Hilchenbach, M., Möbius, E., Canfield, L.R., Vest, R.E., Watts, R., Tarrío, C., Kühne, M., Wurz,

- P., 1998. First Solar EUV Irradiances Obtained from SOHO by the Cielas/Sem. Solar Phys., 177,161–173.
- Lee, C.-K., Han, S.-C., Bilitza, D., Seo, K.-W., 2012. Global characteristics of the correlation and time lag between solar and ionospheric parameters in the 27-day period. J. Atmos. Sol.-Terr. Phys, 77, 219–224, doi:10.1016/j.jastp.2012.01.010.
- Pesnell, W.D., Thompson, B.J., Chamberlin, P.C., 2012. The Solar Dynamics Observatory (SDO). Solar Phys., 275. 3-15, doi:10.1007/s11207-011-9841-3.
- Picone, J.M., Hedin, A.E., Drob, D.P., 2002: NRLMSISE-00 empirical model of the atmosphere: statistical comparisons and scientific issues. J. Geophys. Res., 107, 1468, doi:10.1029/2002JA009430.
- Schmidtke, G., Brunner, R., Eberhardt, D., Halford, B., Klocke, U., Knothe, W., Konz, M., Riedel, W.-J., Wolf, H. 2006: SOL-ACES: Auto-calibrating EUV/UV spectrometers for measurements onboard the International Space Station. Adv. Space Res., 37, 273-282.
- Schmidtke, G., Nikutowski, B., Jacobi, Ch., Brunner, R., Erhardt, Ch., Knecht, S., Scherle, J., Schlagenhauf, J., 2014: Solar EUV irradiance measurements by the Auto-Calibrating EUV Spectrometers (SolACES) aboard the International Space Station (ISS), Solar Phys., 289, 1863-1883, doi: 10.1007/s11207-013-0430-5.
- Unglaub, C., Jacobi, Ch., Schmidtke, G., Nikutowski, B., Brunner, R., 2011: EUV-TEC proxy to describe ionospheric variability using satellite-borne solar EUV measurements: first results, Adv. Space Res., 47, 1578-1584, doi:10.1016/j.asr.2010.12.014.
- Unglaub, C., Jacobi, Ch., Schmidtke, G., Nikutowski, B., Brunner, R., 2012: EUV-TEC proxy to describe ionospheric variability using satellite-borne solar EUV measurements, Adv. Radio Sci., 10, 259-263.
- Woods, T. N., Bailey, S., Eparvier, F., Lawrence, G., Lean, J., McClintock, B., Roble, R., Rottmann, G. J., Solomon, S. C., Tobiska, W. K., White, O. R., 2000: TIMED Solar EUV Experiment, Phys. Chem. Earth (C), 25, 393–396.
- Woods, T. N., Eparvier, F., Bailey, S., Chamberlin, P., Lean, J., Rottmann, G. J., Solomon, S. C., Tobiska, W. K., Woodraska, D. L., 2005: Solar EUV Experiment (SEE): Mission overview and first results, J. Geophys. Res., 110, A01312, doi:10.1029/2004JA010765.
- Woods, T.N., Eparvier, F.G., Hock, R.; Jones, A.R., Woodraska, D., Judge, D., Didkovsky, L., Lean, J., Mariska, J., Warren, H., McMullin, D., Chamberlin, P., Berthiaume, G., Bailey, S., Fuller-Rowell, T., Sojka, J., Tobiska, W.K., Viereck, R., 2012: Extreme Ultraviolet Variability Experiment (EVE) on the Solar Dynamics Observatory (SDO): Overview of Science Objectives, Instrument Design, Data Products, and Model Developments, Solar Physics, 275, 115-143, doi: 10.1007/s11207-009-9487-6.